COMPRESSOR RIG TEST WITH DISTORTED INFLOW USING DISTORTION GENERATORS

J.A. Lieser, Rolls-Royce Deutschland Ltd & Co KG, Dahlewitz, Germany
C. Biela, C.T. Pixberg, H.-P. Schiffer, Technische Universität Darmstadt, Germany
S. Schulze, A. Lesser, C.J. Kähler, R. Niehuis, Universität der Bundeswehr, München, Germany

Summary

At high angle of attack and in ground crosswind operation of an aircraft the turbofan engine is typically exposed to inlet distortions, either generated by the aircraft wing and fuselage or the inlet separation for instance. The need to assess the aircraft engine compatibility in an early stage of engine development is discussed at the beginning of the paper. The main part of the paper is the presentation of a compressor rig test performed at Technische Universität Darmstadt. The setup and motivation of the test, dedicated to address a certain distortion known to occur in rear fuselage nacelles, is explained. A distortion generator was designed by the Universität der Bundeswehr in Munich which was qualified in the present campaign. Special attention was directed towards the characterisation and quantification of the distortions by combining Kulite total pressure measurements and stereoscopic Particle Image Velocimetry in front of the transonic rotor. The Particle Image Velocimetry measurements identified counter-rotating vortex pairs behind the distortion generator which decay rapidly in the accelerating flow in front of the rotor. The Kulite measurements showed the local character of the total pressure distortion and frequency spectra were calculated in the area of vortex shedding. Comparisons of the Kulite measurements in front and behind the rotor demonstrate the changes in shape of the distortion while travelling through the rotor. High resolution measurements of the total pressure ratio used to determine the compressor map show increased pressure ratios accomplished by an increase in total temperature in a sector behind the distortion generator slightly shifted circumferentially in direction of the rotor rotation. Compressor speed lines dropped to a lower pressure ratio caused by the pressure drop of the distortion generator, while the stability was mainly unaffected.

1. INTRODUCTION AND MOTIVATION

Engine certification (JAR-E/FAA-33) and aircraft certification (JAR/FAR 25) are separate processes. Part of the engine certification is the specification and demonstration of compatibility with aircraft requirements ahead of any flight testing. A certified engine may be installed at different aircrafts as long as the compatibility is given. The presented paper deals with the topic of inlet distortions caused either by ingested wakes from the aircraft or high angles of inflow relative to the engine centreline caused by flight manoeuvres and ground crosswind operation. Aircraft flight envelope and ground crosswind requirements result in a maximum level of distortion the engine has to deal with. This level needs to be specified/quantified and the engine will be designed and tested to show stable operability within the specified distortion limits. For the engine manufacture it is therefore important to use appropriate distortion descriptors and a strategy to test the engine which is accurate and cost efficient. Once the engine is certified and flight testing of the aircraft started the aircraft/engine configuration will be certified as a unit according to the rules of JAR/FAR 25. It is important that the customer requirements are met for the certified engines when installed on the aircraft and flight tested.

A generalized way of describing circumferential and radial total pressure distortions is standardized in the SAE document ARP1420 [1]. In the 1960s Rolls-Royce performed a lot of testing of compressors and suggested circumferential critical values (cf. [2]). Distortions concentrated within a circumferential section of 60 degrees were found to cause the most severe stability issues and the so called DC60 value was established and worked well in combination with the parallel compressor theory for many years. DC60 is the ratio of difference in total pressures averaged over the worst 60 degree segment and the complete fan face to the dynamic head at the fan face. An overview of recent developments in parallel compressor theory and distortion descriptors used is given in [3,4]. Using simplified circumferential distortion descriptors assumes a response based on the rotation of the rotor through a fixed distortion area and neglects radial redistribution of distortion. For improved modelling of the time response of the compressor the shape of the distortion is important. In addition to the circumferential shape which is steady in the absolute frame of reference dynamic parts are present, which can add up to one-third to the steady state pressure. If the compressor tends to stall in the near tip region and tip flow becomes important the parallel compressor theories will not be accurate enough and a better understanding of the tip flow is necessary. In [5] a computational method is presented to calculate forced response of a fan due to ground vortex ingestion. Simulating the distortion and fan response within one model makes the use of distortion descriptors

unnecessary. Nevertheless the use of such high fidelity methods is too expensive to be used as a standard tool covering all issues during the engine development program. For a F/A-18A aircraft effects of time variant inlet distortions during aircraft manoeuvres and the resulting engine behaviour were investigated [6]. It is concluded, that stall events of the compressor did not always correlate with the magnitude of the distortion characterized by spatial steady state distortion descriptors. With more advanced fan designs and higher demands on efficiency and safety in the civil sector and manoeuvrability in the military sector Rolls-Royce is therefore investigating more advanced distortion descriptors and simulation technologies. Recently Rolls-Royce performed crosswind testing of a rear fuselage mounted engine using a crosswind blower and fuselage simulator and observed transient behaviour of the distortions. The setup is shown in Figure 1.

Figure 1 Engine certification testing with crosswind blower and fuselage simulator using the Rolls-Royce test facility at Stennis Space Center Mississippi.

During the testing different kinds of distortions were observed which are:

- Large scale vortices behind the fuselage causing swirl and unsteady inflow
- Longitudinal vortices build up on the fuselage (similar to ground vortices)
- Intake shock induced lip separation causing separation bubbles

In the literature several papers can be found dealing with those kinds of distortions. The majority of them are dealing with swirl and longitudinal vortices.

In this paper the characterisation and the effect of separation bubbles in the intake and unsteadiness caused by the fuselage wakes (small scale vortex shedding), on the performance is the main focus. On the rig a vortex generator is used to simulate the vortex shedding. The experiments were performed in the well established compressor rig at Technische Universität (TU) Darmstadt by using standard compressor instrumentation along with unsteady pressure measurement equipment as well as optical measurement techniques such as stereoscopic Particle Image Velocimetry (PIV). The experimental details will be outlined in the following section and the results of the test campaign are discussed in section 3-5.

2. TEST SETUP

All compressor investigations were conducted in the transonic compressor test facility of the TU Darmstadt. The open circuit designed facility sucks ambient air into the compressor via a settling chamber and a flow meter before entering the test section (cf. schematic sketch of the rig in Figure 2).

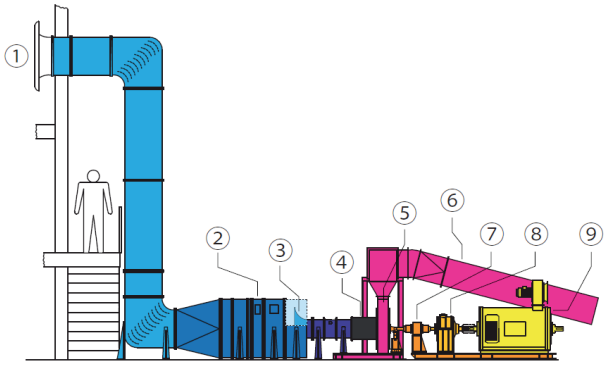

Figure 2 Schematic drawing of the transonic compressor test facility at Technische Universität Darmstadt: 1) Inlet, 2) Settling chamber, 3) Nozzle, 4) Test section, 5) Radial diffusor, 6) Outlet ducting, 7) Torque meter, 8) Gearbox, 9) D/C Drive.

To be able to investigate generic inlet distortions the known research compressor Darmstadt-Rotor-1/Darmstadt-Stator-1 [7] was equipped with a modified casing to hold the distortion generator. The casing section with the distortion generator could be rotated automatically to different circumferentially positions. This was important to obtain the full flow information behind the distortion generator without traversing the PIV measurement plane and the Kulite and to keep the relative position to the stator. The test section depicted in Figure 3 shows the axial position of the distortion generator and the large PIV window. The positions MP1 to MP3 show the measurement planes for the Kulite total pressure sensor. The upstream position MP1 is 75 mm downstream of the distortion generator. A cutaway of the test section in Figure 4 illustrates the build up of the test section. The distortion generator is connected to a ring inside the casing which can be freely positioned by an external actuator. Downstream of the stator five equally distributed rakes in circumferential direction measure total temperature and total pressure at eleven radial positions.

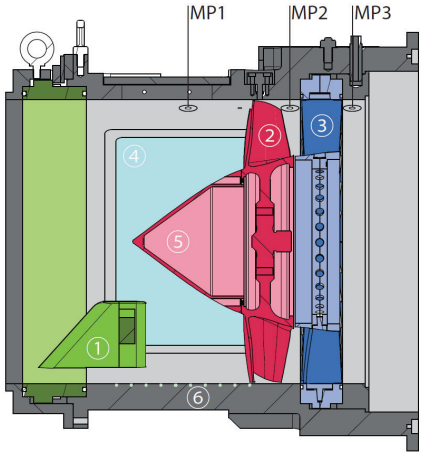

Figure 3 Drawing of the test section: 1) Distortion generator, 2) Darmstadt-Rotor-1, 3) Darmstadt-Stator-1, 4) Plexiglas window, 5) Spinner, 6) Static wall pressure taps (Airflow from left).

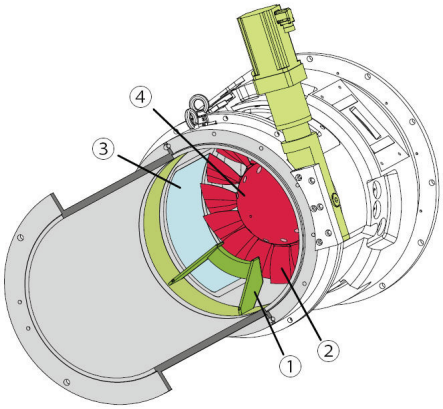

Figure 4 Cutaway of the testsection: 1) Distortion generator, 2) Darmstadt-Rotor-1, 3) Plexiglas window, 4) Spinner.

Circumferential traverses in the facility are realized by traversing the stator vanes relative to the fixed rakes behind the stage. The distortion generator is traversed together with the stator keeping the relative position identical during traverses in a passage. The Kulite total pressure probe is at a fixed circumferential position and traversed in radial direction only while circumferential traverses are realized by traversing distortion generator and stator together. The design of the distortion generator as shown in Figure 4 is described in more detail in reference [8]. The distortion generator was designed to generate vortex shedding with a frequency of 442 Hz at 100% rotor speed and 264 Hz at 65% rotor speed in a circumferential segment of about 60 degree.

The experimental setup of the stereoscopic Particle Image Velocimetry (PIV) system features a Litron Nd:YAG double pulse laser with a pulse energy of 200 mJ and two PCO 4000 double shutter CCD cameras. The light sheet optics were aligned such that a horizontal measurement plane between the distortion generator and the rotor within the compressor rig's symmetry plane could be generated. A flush mounted Plexiglas window in the casing of the test rig was used for the optical access (cf. Figure 5). The repetition rate of the laser was set with a once-per-revolution trigger on the compressor's rotor shaft which results in a measurement related to a fixed blade position. For the measurements tracer particles with a diameter of 1 µm [9] were introduced right in front of the inlet at position 1 in Figure 2.

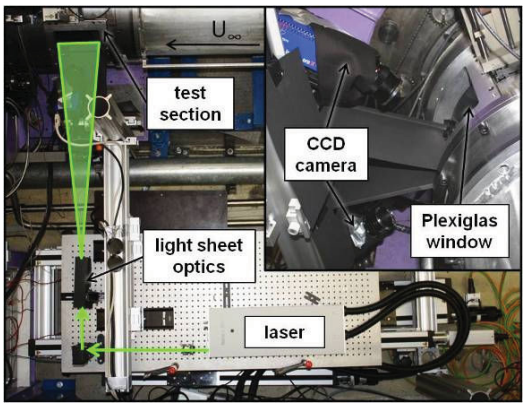

Figure 5 Experimental setup of the PIV measurements.

3. COMPRESSOR PERFORMANCE

The following section describes the approach to determine the compressor speed line with non-uniform inflow. Prior to the distortion generator installation reference measurements without distortion generator were conducted to establish a datum configuration. After this the speed line with distorted inflow was measured in two steps. First, the flow field was mapped for two designated operating points: peak efficiency (PE) and near stall (NS) using a full annulus approach. Then, the rest of the characteristic was measured with lower circumferential resolution.

3.1. High Resolution Measurement

Usually compressor maps are calculated from distributed measurements of pressure and temperature downstream of the compressor stage. The exit flow is believed to be passage-periodic so that the measurement of a single stator passage is sufficient, i.e. representative in order to calculate the compressor operating point. By inserting the distortion generator this assumption is not valid and creates the need for circumferentially resolved flow fields. In this experiment the distortion generator was traversed stepwise around the circumference resulting in an exit flow field of ten measurements per stator passage. Figure 6 and Figure 7 illustrate the total pressure ratio Π and the total temperature ratio Θ at 100% rotor speed PE operating point. Both plots show a clear circumferential variation of the exit flow field. From this data the total pressure ratio of the complete stage can be calculated (see next section for speed line).

A closer look on the exit flow fields shows an increased pressure ratio accompanied by an increase in total temperature rise at the top right sector. This is caused by the altered rotor inflow conditions downstream of the distortion generator which are shifted in circumferential direction by the rotor rotation. During the high-resolution measurements all static ports upstream of the rotor were sampling the static wall pressure for every distortion

generator position. The static wall pressure features a steep gradient in axial direction due to the acceleration of the flow caused by the spinner cross section. To be able to visualise the circumferential pressure distribution Δp_θ was calculated following Eq. (1).

(1) $\Delta p_\theta = (p - \bar{p})/\bar{p}$

Here p is the static pressure at a given position and $\bar{p}$ is the circumferential average of the pressure which varies only in axial direction.

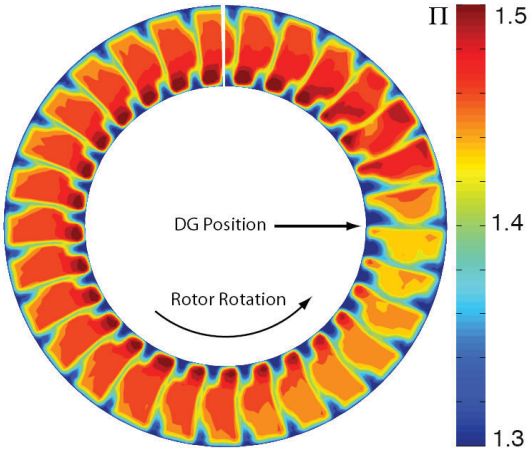

Figure 6 Contourplot of total pressure ratio distribution downstream of stator at 100% shaft speed, peak efficiency operating point, view upstream behind stator.

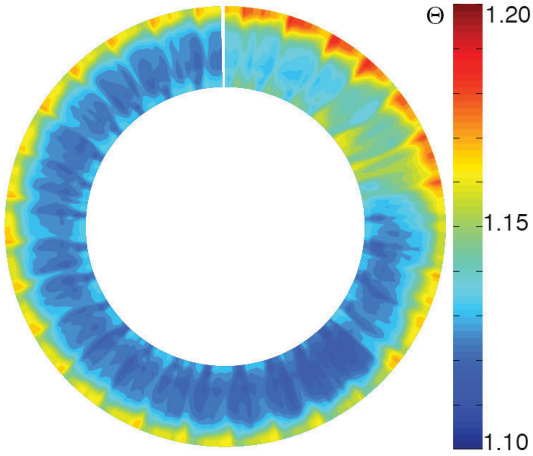

Figure 7 Contourplot of total temperature ratio distribution downstream of stator at 100% shaft speed, peak efficiency operating point, view upstream behind stator.

Figure 8 shows the static pressure variation at peak efficiency operation of the transonic compressor. At around ninety degrees the footprint of the distortion generator is clearly visible. It is also easily seen, that the footprint of the distortion generator is widely mixed out before it enters the rotor plane and that the rotor influences the flow upstream of the rotor causing a non-symmetric static pressure distribution.

Since the measurement of a full annulus is time costly only two operating points could be measured with high resolution.

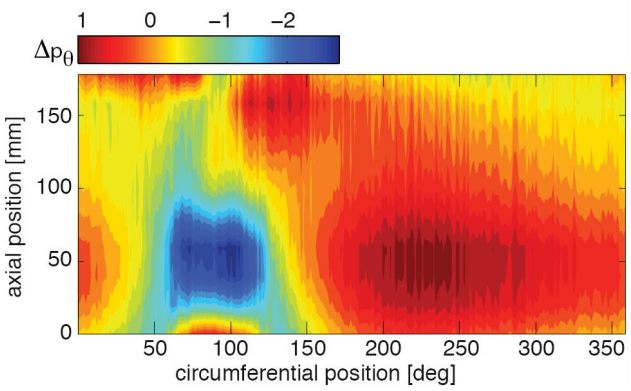

Figure 8 Contourplot of the static pressure variation on the casing wall upstream of the rotor. Flow is coming from the bottom, last pressure is measured at leading edge of rotor.

3.2. Low Resolution Measurement

To reduce the testing time the 100% speed line was calculated from five equally distributed stator passage measurements, where one passage was placed just downstream of the distortion generator. The total pressure ratio of each passage was calculated and the results averaged. Figure 9 shows the resulting compressor speed line. The green squares represent the full annulus measurements discussed in the previous section. The red line depicts the five passage average. To visualise the circumferential variation small symbols indicate the value of each passage for the respective massflow.

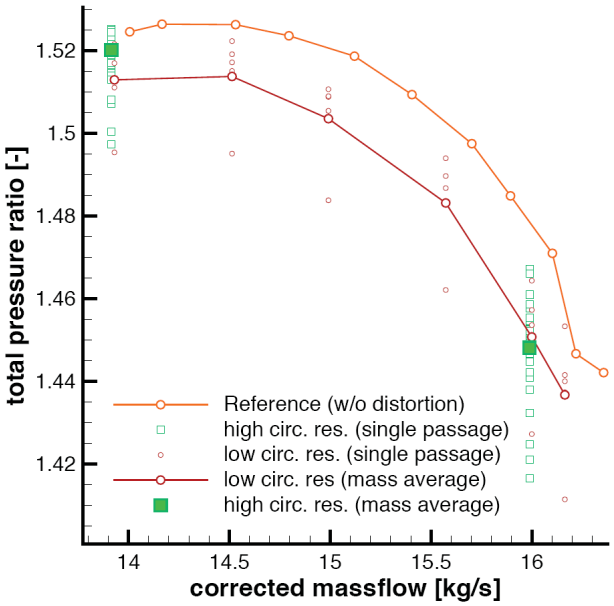

Figure 9 Total pressure ratio versus corrected massflow for 100% rotor speed line.

A reduction of the compressor stability is not visible. Moreover, the trend of the red speed line is comparable to

the undistorted reference case (amber line) with an overall reduced pressure ratio which is possibly caused by the total pressure drop downstream of the distortion generator. At PE the five-passage-average is close to the two full annulus measurements while at NS the full annulus measurement shows a higher pressure ratio. By comparing the distribution of the high resolution results with the low resolution average it can be seen, that the measurements in the passage downstream of the distortion generator are overweighted by the five-passage average at NS condition.

4. PARTICLE IMAGE VELOCIMETRY

In order to gain more insight into the flow structure behind the distortion generator stereoscopic Particle Image Velocimetry (PIV) measurements were conducted with the measurement setup described in chapter 2. Figure 10 shows the positions of the five investigated measurement planes relative to the distortion generator. Special emphasis was put on the near stall and peak efficiency operating points for the 65% and 100% characteristics. But also other massflow rates between near stall and peak efficiency were analyzed.

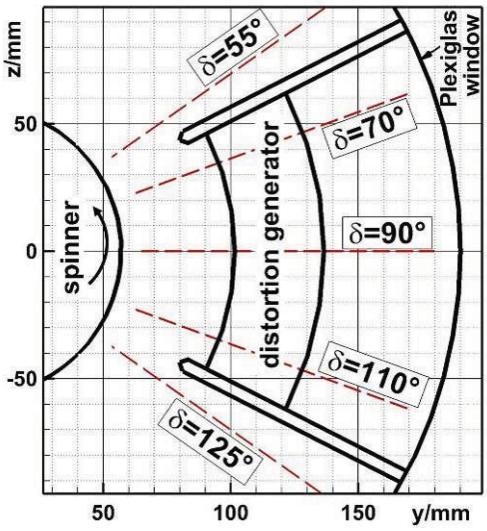

Figure 10 Measurement plane positions behind the distortion generator, view upstream.

In Figure 11 averaged vector fields are shown for the five different positions behind the distortion generator. The flow first approaches the distortion generator plotted on the left hand side of each figure and continues afterwards towards the rotor plane on the right hand side. The operating point is peak efficiency of the 100% characteristic at a true massflow rate of 12.14 kg/s. The background color depicts the value of the velocity component in the axial direction. Blue regions thus represent areas of reversed flow. In general it can be seen that the flow is accelerated towards the rotor plane since the spinner causes a reduction of the test rig cross-section. The area of reversed flow is largest in the middle of the distortion generator (δ = 90°, about 62 mm length) and decreases towards the side edges of the generator. Note that the measurement planes δ = 70° and δ = 110° are shifted equally from the middle of the distortion generator to both sides. The areas of reversed flow however differ slightly to the symmetrical geometry. The reason for this deviation is the influence of the rotating spinner and the rotor blades. The area of reversed flow for δ = 70° is always a little smaller than the according area for δ = 110°.
Within a characteristic the size of the area of reversed flow is also dependent on the true mass flow rate in the test rig. The higher the true mass flow rate is the bigger the region of reversed flow becomes (not shown here).

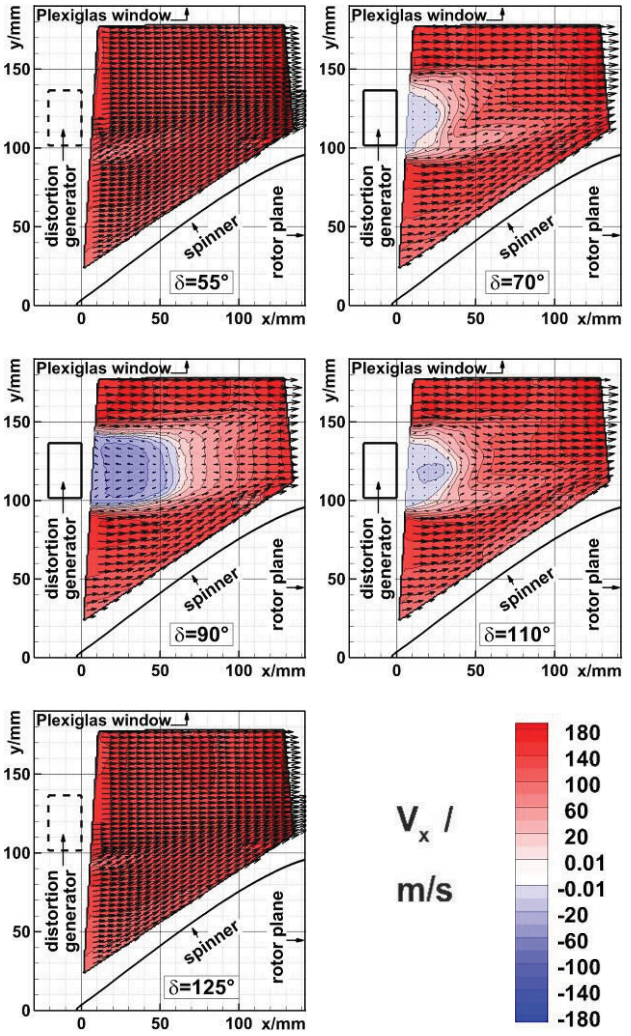

Figure 11 Regions of reversed flow for different positions behind the distortion generator, peak efficiency, 100%, m_{true} = 12.14 kg/s.

The effect of the rotational movement of the spinner and rotor blades can also be observed in Figure 12 where the turbulent kinetic energy is displayed for all investigated positions behind the distortion generator. The exemplary operation point again is peak efficiency of the 100% characteristic at a true mass flow rate of 12.14 kg/s. The utmost measurement planes outside of the distortion generator (δ = 55°, δ = 125°) are still affected by the generator body, and the influence of rotating spinner and blades can also be observed. The values of turbulent kinetic energy for all investigated operation points are in general higher for the outer measurement planes in the direction of rotation (δ = 55°) than for the planes in the opposite direction (δ = 125°). Also the vortices are carried further downstream close to the spinner than close to the

Plexiglas window at δ = 70° and 110°. The authors hope for a more comprehensive insight into this 3D flow problem as soon as the numerical simulations for this setup will be available.
Furthermore Figure 12 shows discontinuities close to the test rig wall where the Plexiglas window is situated at approximately x = 31 mm and x = 84 mm. These discontinuities are due to the transonic operating point of the compressor. Here shocks form at every single rotor blade and proceed upstream. The abnormality of the flow field around x = 105 mm and y = 100 mm is a consequence of reflections at the spinner's surface which in the future can be avoided by applying special fluorescent paint on all surfaces and using suitable filters in front of the cameras.

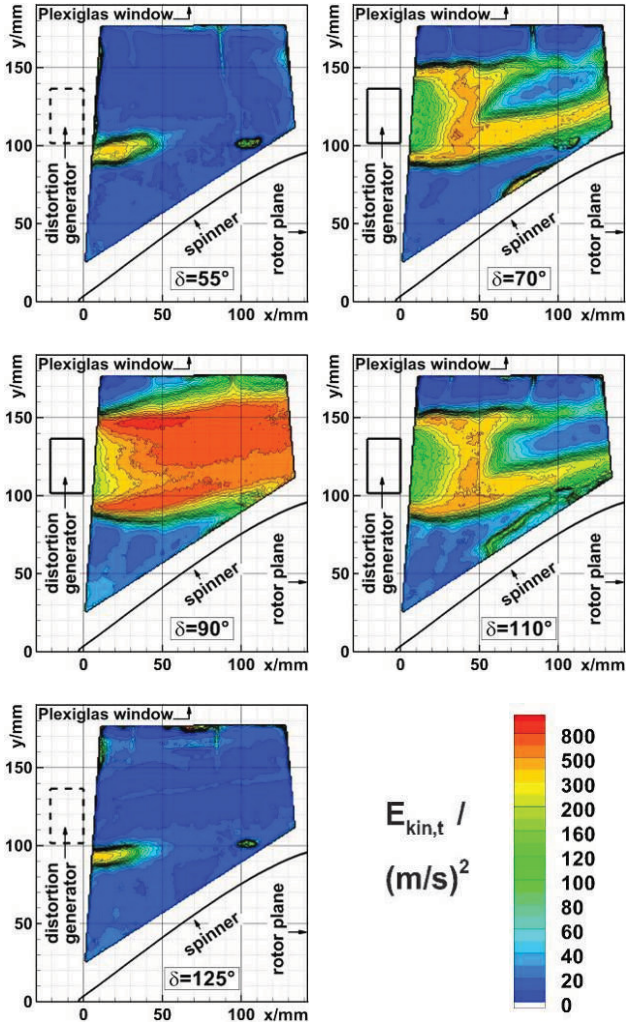

Figure 12 Turbulent kinetic energy for different positions behind the distortion generator, peak efficiency, 100%, m_{true} = 12.14 kg/s.

The distortion generator was analytically designed to show a vortex shedding with a frequency of 442 Hz, and pre-experiments in a blow-down wind tunnel at the Universität der Bundeswehr in Munich with a simplified distortion generator and a time-resolved PIV system yielded a characteristic frequency in the order of magnitude of 419 Hz in the middle of the distortion generator (cf. Lesser et al. [8]). In the experiments described in this paper no time-resolved PIV system was applied. Therefore the characteristic frequency of the vortex shedding was estimated by determining the distance d between two counter-rotating vortices and their convection speed U_w. Thus the frequency of the vortex street is calculated from Equation (2):

(2) $f=U_w/d$

Figure 13 shows such a counter-rotating vortex pair from an instantaneous vector field which is typical for the distortion generator's vortex street. From a variety of instantaneous vector fields a characteristic frequency between 390 Hz and 500 Hz was found by this means for equally rotating vortices. A comparison with the intended 442 Hz proofs that the design of the vortex generator in this aspect was successful.

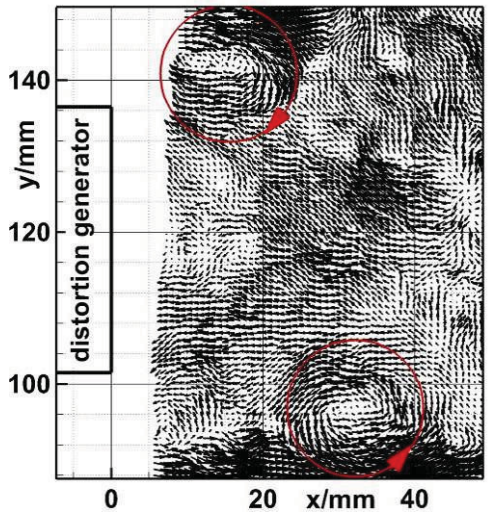

Figure 13 Vortices behind the distortion generator, peak efficiency, 100%, m_{true} = 12.14 kg/s.

In Figure 14 an entire instantaneous flow field is shown for peak efficiency of the 100 % characteristic. The coloring depicts the absolute value of the velocity vectors, and it can be stated that the large scale coherent vortices decay before they even reach the rotor plane. This can also be assumed by looking at the size of the area of reversed flow which hardly expands over half the distance between distortion generator and rotor plane (cf. Figure 11). However, the interference of the distorted flow with the compressor's stage is still significantly in agreement with the measurements in Figure 6 and Figure 7. The results obtained from the stereoscopic PIV measurements give detailed insight into the 3D topology of the flow field, induced by the distortion generator, the distribution and intensity of the turbulence and the frequency of the coherent vortices. This information is valuable for the validation of numerical flow simulation techniques but also for designing distortion generators with other properties.

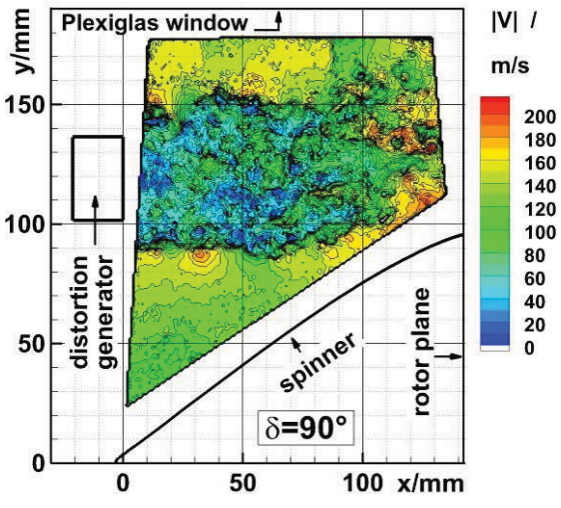

Figure 14 Instantaneous vector field, peak efficiency, 100%, m_{true} = 12.14 kg/s.

5. UNSTEADY PRESSURE MEASUREMENTS

For the performance and the stability of the compressor the time dependence of the flow features behind the distortion generator, which were detected in the PIV measurements, may be of importance. To get additional information about the time behaviour the unsteady total pressure was measured 75 mm downstream of the distortion generator. The total pressure probe setup was already described in chapter 2. The measuring points are shown in Figure 15. The flow field is resolved in circumferential direction at midspan with 24 equidistant points and at four circumferential positions also with 8 radial points. The PIV results show that the flow downstream of the distortion generator is almost symmetric in the circumferential direction of the distortion generator, therefore circumferential symmetry was assumed and for radial investigation the same planes as for the PIV measurement at 90°, at 70°, 55° and 270° were chosen. The different planes were positioned to catch the unsteady flow behaviour in the centreline as well as in the peripheral zones behind the distortion generator. The 270° plane was appended to get the flow features in the most undistorted sector.

The time averaged circumferential total pressure distribution at midspan is shown in Figure 16. The time averaged total pressure upstream of the rotor shows a drop between 60° and 120° with a maximum extent of 15% related to the total pressure in the undistorted sector. Outside of this sector the total pressure remains non-affected. The shape of the total pressure distortion is deflected quantitatively as well as qualitatively when passing the rotor. An undulation with a negative maximum of 3% and a positive maximum of 1% can be observed, instead of the trough shape in front of the rotor.

The time averaged radial total pressure variations in front of the rotor depicted in Figure 17 are in agreement with the PIV measurements displayed in Figure 11. An arc shaped total pressure loss from 20% till 80% span with a maximum extent of 15% of undistorted total pressure level can be observed in the 90° plane. In the 70° plane the total pressure shape shows two local maxima of 5% and 9% of undistorted total pressure, respectively. The total pressure level is the same near hub, at midspan and near casing. No significant influence of the distortion generator is observed near at 55°. Also downstream of the rotor the radial total pressure distribution shows only a slight variation of the pressure profile.

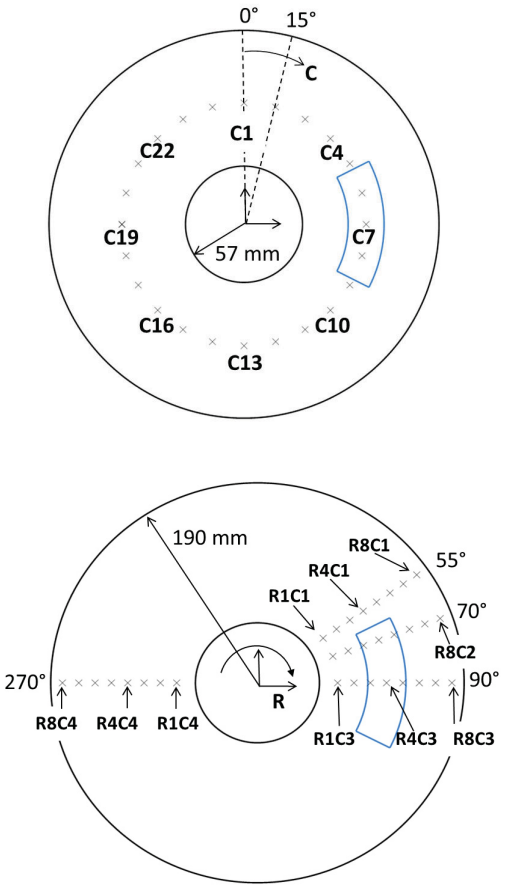

Figure 15 Map of the Kulite measurement points

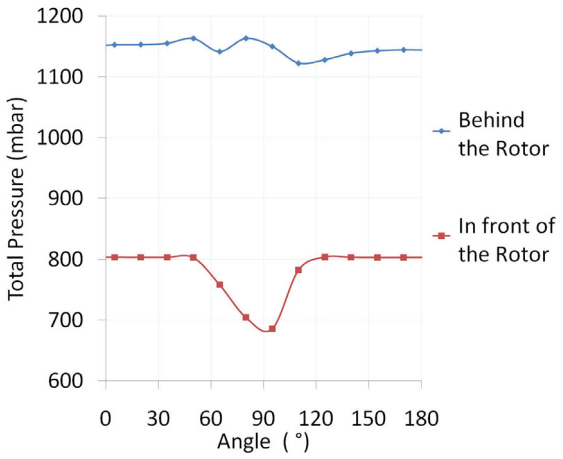

Figure 16 Circumferential total pressure distribution

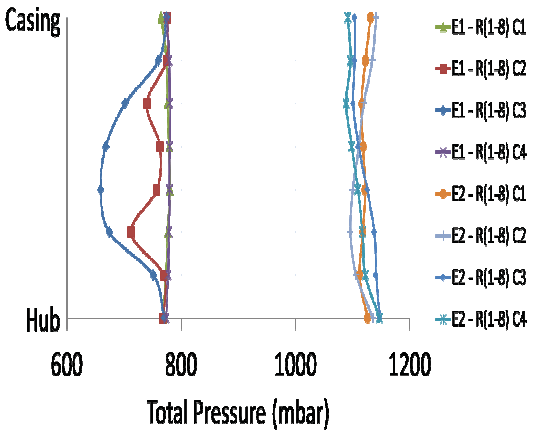

Figure 17 Radial total pressure distribution (E1: in front of rotor, E2: behind the rotor; C1: 55°, C2: 70°,C3: 90°, C4: 270°).

The aim of this investigation was to study the influence of an unsteady intake distortion and the compressor response. Therefore the distortion generator was designed to produce unsteady distortions with well-defined frequencies. In Figure 18 the frequency spectrum of measurement point R6C3 is shown. The probe was designed to avoid vibrations in relevant frequencies. The time signal of the Kulite total pressure probe was Fourier transformed using a Cooley-Tukey algorithm [10] and a Hamming window function. Two strong peaks can be observed. The blade passing frequency which is characterized by a very sharp peak, as the blade passing frequency is mechanically constant, and a second peak at 600 Hz which shows flat rising and falling edges. As shown in Figure 13 the distortion generator sheds a vortex pair at the upper and lower edge, respectively. The frequency of 600Hz is in the order of the shedding frequency of the upper vortex. The difference between the frequency obtained by PIV results and the total pressure measurement results is due to the different axial positions. The vortices shed by the distortion generator decay into smaller vortices as traveling downstream leading to a broadening of the peak and a shift to higher frequencies.

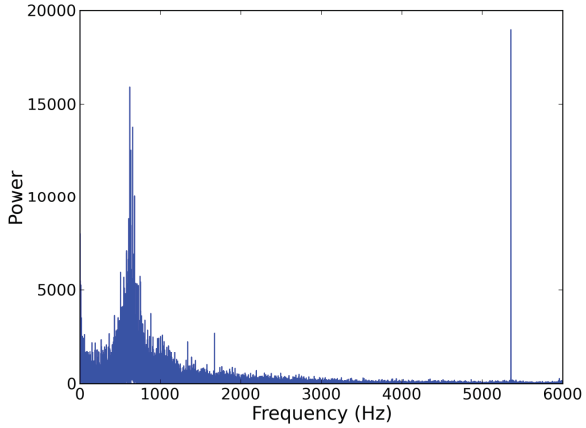

Figure 18 Frequency spectrum of the total pressure variation of measurement Point R6C3.

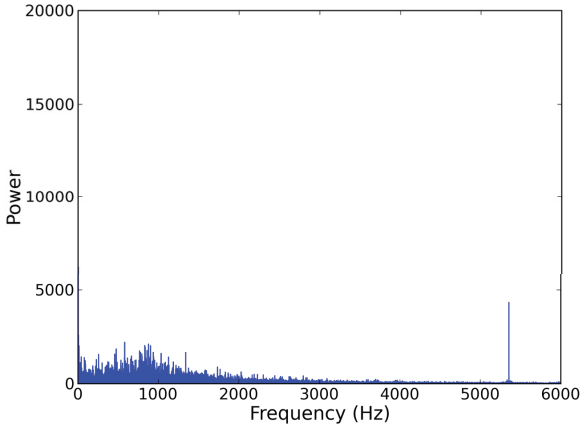

Figure 19 Frequency spectrum of the total pressure variation of measurement Point R3C3.

In Figure 19 the frequency spectrum of measurement point R3C3 is shown. Although both peaks that were observed at measure point R6C3 exist they are less pronounced.

6. CONCLUSIONS AND OUTLOOK

The paper presents the results of a generic rig test to simulate unsteady inlet distortions and their influence on a transonic compressor stage. One of several possible kinds of distortions was chosen to show the feasibility of the rig and measurement techniques to gather all important information for better understanding of the fan distortion interaction and validation of numerical methods. The test was supposed to focus on aerodynamic phenomena and blade vibrations were avoided, which was monitored by the rigs tip timing system.

The TU Darmstadt compressor rig was successfully modified for generation and detailed measurements of the distorted inflow. The mechanical design and traverse control in the facility allows reproducible measurements. The window for the PIV measurements was sufficiently large and small vibrations did not lower the measurement accuracy.

Due to the nature of the distorted flow pattern it is not sufficient to determine the compressor maps total pressure ratio by traversing one passage only as it is done in case of undistorted inflow. A high resolution traverse was done for peak efficiency and near stall on the 100% speed line only and compared to low resolution measurements. While for peak efficiency the results compare quite well the drop of the speed line is over estimated with the low resolution method at near stall condition. The drop of speed line is nearly constant, corresponding to the pressure drop of the distortion, and compressor stability is not affected.

Spatial and transient behaviour of the distortion in front of the rotor could be described by combining stereoscopic PIV and Kulite measurements. As shown by the PIV and Kulite measurements the total pressure distortion was locally focused on a 60 degree segment and midspan of the rotor. The axial development in front of the rotor was

captured by the PIV measurements and showed a decay of vortices shed by the distortion generator before they reached the rotor face. In the tests of the distortion simulator in a wind tunnel without a rotor/spinner and constant mean flow speed the decay moved further downstream. Kulite total pressure measurements were performed at an axial station upstream and downstream of the rotor. The amplitude of the distortion decreased in the rotor and the shape changed from a trough shape to a wavy shape with two local minima. Characteristic frequencies derived from the PIV measurements correspond to the design of the distortion generator and isolated measurements. The Kulite measurements were taken at an axial station further downstream where the vortices already changed in amplitude and frequencies leading to broadened spectra with a maximum at a shifted frequency.

Concerning the intake/fan compatibility strategy the resultant distortion and its effect on the compressor working line in the present campaign would justify the use of a steady state total pressure distortion descriptor. Low resolution measurements with one rake per passage for the compressor or one rake per 60° segment for the distortion may lead to an overestimation of the working line drop as shown by comparison between high and low resolution measurements. Since the rig is not fully representative for an engine intake and spinner contour the high dissipation of the vortices due to the presence of the compressor stage may not be generalized for engines. Nevertheless the test is simulated by CFD within the DFG research group and the data presented here will be used for comparison and validation of the numerical method. Once the numerical methods are validated a more realistic engine configuration may be investigated by means of numerical simulations to assess the effect of the fan on the level of distortions.

For an engine the change in stability line is more important since the working line drop and thrust decrease due to distortions may be compensated by the engine control system. In the proposed follow-on program the distortion will therefore be increased by moving the generator closer to the rotor and the distortion will focus on the blade tip. The used rotor 1 of the TU Darmstadt rig is sensitive to tip flow disturbance and in the next campaign the aim is to significantly drop stability margins by affecting the tip vortex. Numerical simulations of intakes in crosswind will support the design of additional distortion generators representing typical flow patterns such as vortex shedding and swirl. The follow-on test will further support the long term objective to find out if DC60 type of distortion description used in isolated rig tests of intake and compressors today is sufficient for distortions as seen during the engine tests in Stennis.

ACKNOWLEDGMENTS

The authors gratefully acknowledge the support of the “Deutsche Forschungsgemeinschaft DFG” (German Research Foundation) and thank Rolls-Royce Deutschland Ltd & Co KG for the permission to publish this paper.

REFERENCES

[1] Aerospace Recommended Practice (ARP) 1420: “Gas Turbine Inlet Flow Distortion Guidelines”, Society of Automotive Engineers, 2002.

[2] J. Seddon, E.L. Goldsmith: “Intake Aerodynamics”, Collins, 1985.

[3] W.T. Cousins, M.W. Davis: “Evaluating Complex Inlet Distortion with Parallel Compressor Model: Part 1 – Concepts, Theory, Extensions and Limitations”, ASME Turbo Expo, GT2011-45067, June 6-10, 2011.

[4] M.W. Davis, W.T. Cousins: “Evaluating Complex Inlet Distortion with Parallel Compressor Model: Part 2 – Applications to Complex Patterns”, ASME Turbo Expo GT2011-45068, June 6-10, 2011.

[5] L. Mare, G. Simpson, A.I. Sayma: “Fan Forced Response due to Ground Vortex Ingestion”, ASME Turbo Expo GT2006-90685, May 8-11, 2006.

[6] W. G. Steenken, J.G. Williams, A.J. Yuhas, K.R. Walsh: “An Inlet Distortion Assessment During Aeircraft Departures at High Angle of Attack for an F/A-18A Aircraft”, NASA TM 104328, 1997.

[7] G. Schulze, C. Blaha, D.K. Hennecke and J.M. Henne: “The Performance of a New Axial Single Stage Transonic Compressor”, ISABE, 95-7072, Melbourne, Australia, September 10-15, 1995.

[8] A. Lesser,S. Schulze, R. Niehuis, C.J. Kähler, J. Lieser: “Analytical Design of an Inlet Distortion Generator and its Experimental and Numerical Validation”, to be published in series: Notes on Numerical Fluid Mechanics and Multidisciplinary Design: New Results in Numerical and Experimental Fluid Mechanics VIII, Springer, 2011.

[9] Kähler, CJ; Sammler, B; Kompenhans, J: “Generation and control of tracer particles for optical flow investigations in air”, Experiments in Fluids Volume: 33 Issue: 6, Pages: 736-742.

[10] James W. Cooley, John W. Tukey: “An algorithm for the machine calculation of complex Fourier series”. In: Math. Comput. 19, 1965, S. 297–301.